Original Research Article

Dosimetric comparison of automatically propagated prostate contours with manually drawn contours in MRI-guided radiotherapy: A step towards a contouring free workflow?

Kobika Sritharan [a,b,*], Alex Dunlop [c], Jonathan Mohajer [c], Gillian Adair-Smith [a], Helen Barnes [a], Douglas Brand [b], Emily Greenlay [a], Adham Hijab [a,b], Uwe Oelfke [c], Angela Pathmanathan [a,b], Adam Mitchell [c], Julia Murray [a,b], Simeon Nill [c], Chris Parker [a,b], Nora Sundahl [a,b], Alison C. Tree [a,b]

[a] *The Royal Marsden NHS Foundation Trust, United Kingdom*
[b] *The Institute of Cancer Research, United Kingdom*
[c] *The Joint Department of Physics, the Royal Marsden Hospital and the Institute of Cancer Research, United Kingdom*

ARTICLE INFO

ABSTRACT

Background: The prostate demonstrates inter- and intra- fractional changes and thus adaptive radiotherapy would be required to ensure optimal coverage. Daily adaptive radiotherapy for MRI-guided radiotherapy can be both time and resource intensive when structure delineation is completed manually. Contours can be auto-generated on the MR-Linac via a deformable image registration (DIR) based mapping process from the reference image. This study evaluates the performance of automatically generated target structure contours against manually delineated contours by radiation oncologists for prostate radiotherapy on the Elekta Unity MR-Linac.
Methods: Plans were generated from prostate contours propagated by DIR and rigid image registration (RIR) for forty fractions from ten patients. A two-dose level SIB (simultaneous integrated boost) IMRT plan is used to treat localised prostate cancer; 6000 cGy to the prostate and 4860 cGy to the seminal vesicles. The dose coverage of the PTV 6000 and PTV 4860 created from the manually drawn target structures was evaluated with each plan. If the dose objectives were met, the plan was considered successful in covering the gold standard (clinician-delineated) volume.
Results: The mandatory PTV 6000 dose objective (D98% > 5580 cGy) was met in 81 % of DIR plans and 45 % of RIR plans. The SV were mapped by DIR only and for all the plans, the PTV 4860 dose objective met the optimal target (D98% > 4617 cGy). The plans created by RIR led to under-coverage of the clinician-delineated prostate, predominantly at the apex or the bladder-prostate interface.
Conclusion: Plans created from DIR propagation of prostate contours outperform those created from RIR propagation. In approximately 1 in 5 DIR plans, dosimetric coverage of the gold standard PTV was not clinically acceptable. Thus, at our institution, we use a combination of DIR propagation of contours alongside manual editing of contours where deemed necessary for online treatments.

Introduction

The advent of hybrid MRI-linear accelerators has altered the scope of image guided radiotherapy for pelvic tumours. The anatomy within the pelvis demonstrates inter- and intra-fractional changes over the course of radiotherapy treatment. The prostate gland can rotate and deform, it can move relative to the seminal vesicles (SV), its position can be altered by changes in surrounding organs such as the bladder and rectum, and the prostate volume can change as a direct result of radiation treatment [1]. Current image guided techniques with fiducials and/or cone beam computed tomography (CBCT) only account for some of these changes [2,3].

The Elekta Unity MR-Linac (Elekta AB, Stockholm, Sweden) combines a 1.5 T magnetic resonance scanner and a 7MV linear accelerator.

The MR-Linac provides superior soft tissue contrast and the ability to adaptive replan online.

The current workflow on the MR-Linac for treating prostate cancer takes longer than treatment on a standard C-arm Linac (e.g. 45 min vs 10–15 min) and requires a larger multi-professional team to deliver [4]. One of the bottlenecks in the workflow is the time taken for manual contouring of the target and organ at risk (OAR) structures [5,6]. The longer the treatment takes, the greater the risk of intrafraction target motion [7] which, without tracking, can offset the benefits of plan adaptation, hence accelerating the workflow will improve accuracy as well as efficiency.

The use of propagated contours, created automatically by deforming a set of gold standard contours onto the anatomy visualised on daily imaging, is desirable for adaptive radiotherapy as it removes the need for a radiation oncologist or radiographer presence to contour, and thus reduces the fraction delivery time [8,9]. Inter- and intra-observer variability is recognised in prostate cancer contouring [10,11] and use of propagated contours has the potential to reduce the risk of human error as well as variability associated with multiple observers' contouring [12,13].

There are multiple techniques for autosegmentation available; intensity, shape modelling and atlas-based autosegmentation [14]. The latter is widely used in commercially available autosegmentation programmes. The Monaco treatment planning system (TPS) uses a proprietary image registration algorithm and deformable image registration (DIR) based contour propagation occurs through an iterative optimisation process utilising voxel-based information [5,15].

This study aims to compare the accuracy of propagated contours of the prostate and SV with manually drawn contours and assess their suitability for MRI-guided adaptive radiotherapy treatment of localised prostate cancer utilising the existing tools available within the MR-Linac workflow. The primary question of interest is whether a plan created from automated contours delivers adequate dose to the target, as defined by clinician-created contours.

Methods

MRI-guided radiotherapy (MRIgRT) protocol for prostate cancer

Patients with intermediate or favourable high risk localised prostate cancer were recruited to the Prostate Radiotherapy Integrated with Simultaneous MRI (PRISM) trial (NCT0365825) [16,17] which assesses the technical feasibility of delivering radical radiotherapy using the MR-Linac. Patients received a total dose of 6000 cGy in 20 fractions over 4 weeks to the prostate, with a lower dose of 4860 cGy in 20 fractions to the prophylactic SV target. An 'adapt-to-shape' (ATS) strategy was adopted for treatment planning, requiring recontouring of structures and plan optimisation [18,19]. Six months of androgen deprivation therapy (ADT) was given to all patients and commenced approximately 3 months prior to having radiotherapy.

All patients had pre-treatment CT and MRI planning scans. The Monaco (Elekta AB, Stockholm, Sweden, v5.40.00) TPS was used to create the MR-Linac reference plan prior to commencement of the treatment course and for online treatment planning on the Unity MR-Linac as described in Dunlop et al [20]. At the start of each fraction, the standard pelvic T2-weighted MRI Elekta sequence is acquired, called the session image. Target regions of interest (ROIs) and OARs were propagated from the reference to daily session image using either the rigid registration (RIR) based on the prostate position [19] or DIR between the two image sets. RIR mimics the delivery of non-adaptive radiotherapy with standard image-guidance.

The reference image for fraction 1 is the pre-treatment CT planning scan. There is greater accuracy of propagated contours from MR to MR when compared to CT to MR [6,10] and for fraction 2 onwards, the fraction 1 session MRI is implemented as the reference image. The target structures (prostate and SV) were propagated by RIR and the OAR contours were propagated by a combination of RIR (bladder) and DIR (rectum, bowel and penile bulb).

A team of 8 clinicians were responsible for contouring on a rotational basis, having completed a departmental quality assurance programme. The clinician of the day reviewed the propagated target contours, and it is at the clinician's discretion whether to delete and recontour or edit these contours. During fraction one, the target structures are deleted and recontoured on the session image by one of the team and these are used as the reference structure set for future treatments. Occasionally, the OAR contours would require editing if they had not propagated satisfactorily. The clinical target volume (CTV) and planning target volume (PTV) structures are then generated as per the PRISM protocol [16]. All patients in this study had the proximal 2 cm of their SV treated.

Following ROI contouring on the session image, a new plan on the daily image was optimised, and if the mandatory constraints were met for the planning target volumes (PTVs) and OARs, the daily adaptive plan was accepted. A verification MR image to identify any intra-fractional anatomical changes was acquired, and, if required, a positional shift applied before plan delivery.

Patient selection

Ten patients (median age = 73.5 years, range 61–76 years) who had radiotherapy for localised prostate cancer in the PRISM trial at a single institute were selected retrospectively. Four fractions from each patient (fractions 5, 10, 15 and 20) were chosen. The first seven patients enrolled in the PRISM trial were excluded from this study as in patient 8 onwards, scripting was used to create the PTV structures in a consistent manner. The ten selected patients were treated sequentially on the MR-Linac.

Target generation and dose constraints

The 'CTV_prostate' CTV encompasses the prostate and the proximal 1 cm of the SV, and the CTV prostate and SV structure (CTpsv) includes the proximal 2 cm of the SV. The primary planning target volume (PTV 6000) is created by expanding CTV_prostate isotropically by 5 mm except posteriorly, which is grown by 3 mm. The lower dose elective PTV (PTV 4860) is created by expanding CTVpsv by 5 mm isotropically.

Dose analysis

The gold standard for each fraction in this study were the contours outlined by the radiation oncologist on the day of treatment. Each fraction was reviewed offline for any significant contouring errors that may have occurred during online treatment. If present, these contours were excluded.

All structure propagations and dose analyses for this study has been carried out on the Monaco TPS. For each fraction, two copies of the session MR were made (Fig. 1). The prostate was propagated to one copy of the session image by DIR and to the second copy by RIR from the corresponding reference image. For all fractions, the RIR, which requires soft tissue matching to the prostate, was carried out by an MR-experienced therapeutic radiographer. The SV can show significant inter-fraction motion and from clinical experience, RIR was felt to be inappropriate for propagation; the SV were therefore propagated by DIR for both copies of the session image. Once the target structures had been propagated, the PTVs were generated as described by the PRISM protocol. Any OAR structures that had been edited on the day of treatment by the radiation oncologist were copied to the duplicates of the session images, thus the OAR contours were identical for all three plans. Mandatory OAR constraints were prioritised over target coverage.

Two plans, in addition to the gold standard treatment plan, were created: a 'deformable plan' and a 'rigid plan'. Any alterations to the planning optimisation parameters for the online clinical plan were replicated during planning for the propagated contours to minimise any
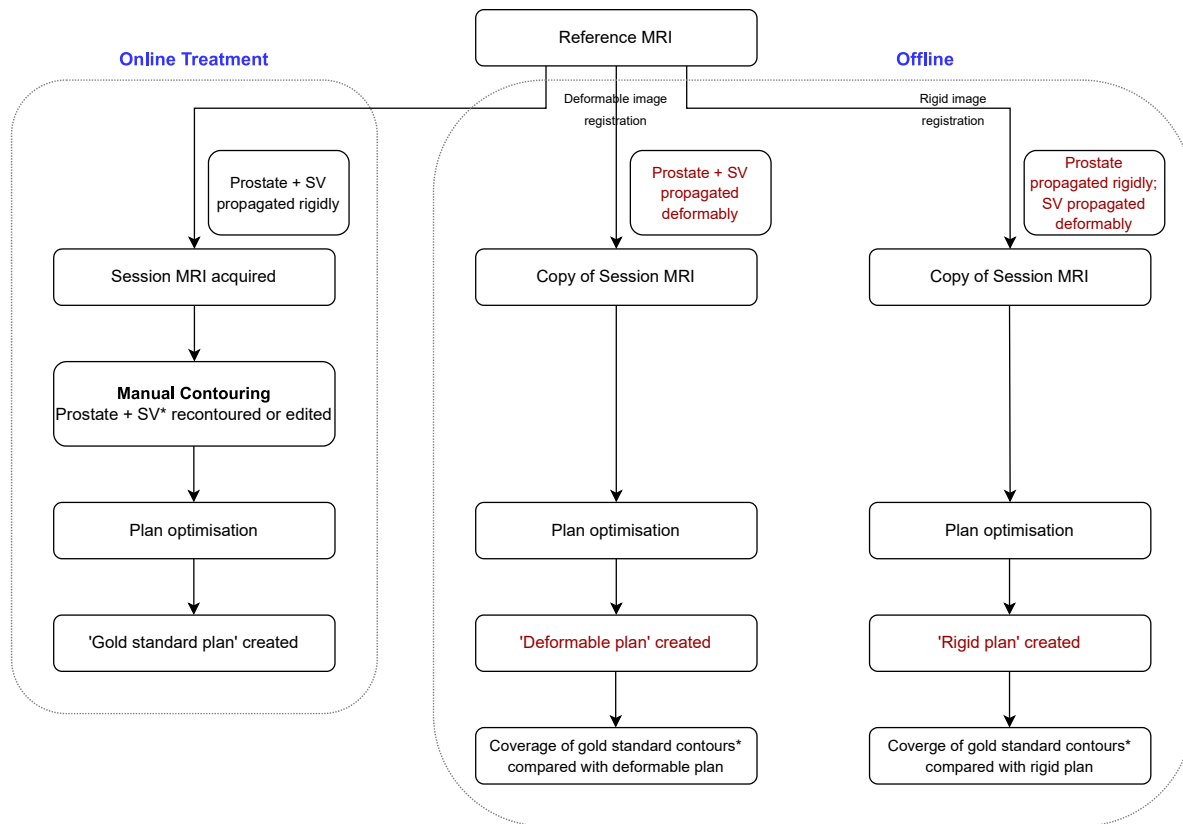
Fig. 1. Schematic of the methodology. Each deformable and rigid plan created was used to assess coverage of the gold standard contours, which are the manual contours drawn during the original treatment (denoted by *).

impact these may have on the results. The deformable and rigid plans were reviewed against the mandatory dose constraints (Table 1). If the plan created was unable to meet the mandatory constraints, it would be deemed not to be suitable for a clinician-free workflow, and thus excluded from the next stage of the analysis.

The dose coverage of the gold standard PTV 6000 and PTV 4860 was then calculated for each fraction with each rigid and deformable plan (Fig. 2). The plan would be considered clinically acceptable if all the mandatory dose constraints (Table 1) for the PTV structures and OARs were met (Table 1, Supplementary file).

Statistics

Target variables have been expressed as proportions with confidence intervals, as they were dichotomised into clinically acceptable (if all mandatory dose constraints were met), or not. Fisher's exact tests were used to compare the rigid plan group and deformable plan group with

each other, as well as each with the gold standard group. A conservative Bonferroni correction was applied to account for multiple testing, thus statistical significance was reached if a value of $p < 0.0167$ was achieved.

Coverage analysis

The deformable and rigid plans which were considered clinically unacceptable, as defined above, were included in this part of the study. These plans were visually inspected for a systematic pattern of under-coverage of the gold standard PTV 6000. To assess this, the PTV 6000 was divided into twelve segments as demonstrated in Fig. 3; a virtual vertical line divided the PTV structure into anterior and posterior segments and horizontally into three sections from top to bottom. The 5700 cGy isodose from each deformable and rigid plan was charted onto the PTV 6000 gold standard contour and on visual inspection, segments of the PTV that were not adequately covered were noted.

Results

Forty fractions in total were analysed from 10 patients. Adverse anatomy resulted in individualised constraints being created for one patient and the same constraints were used when creating the respective deformable and rigid plans.

Two fractions were excluded from the analysis as, at offline review of the clinician contours, the target structures were overly generous. In total 38 fractions were included and a total of 38 deformable and 38 rigid plans were created. Two deformable plans were not included in the final analysis against the clinician contours as these plans did not meet all the mandatory dose objectives de novo hence would not have been used clinically.

Table 1
Dosimetric criteria for the primary and secondary PTVs are shown. Optimal and mandatory targets are outlined in the last column. The mandatory dose constraints must be achieved for the plan to be acceptable.

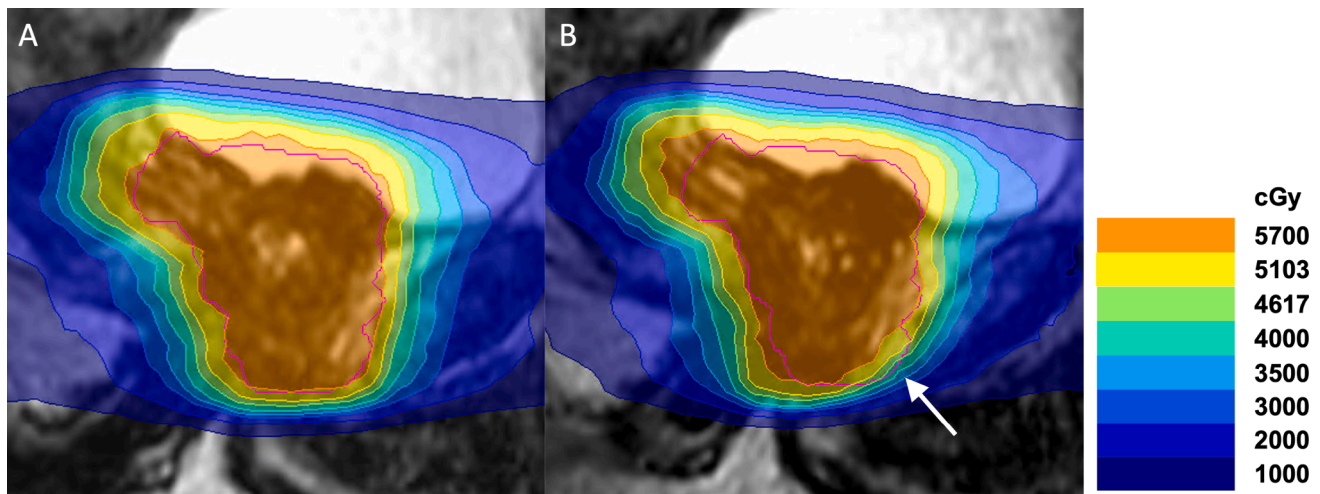| Structure	Dosimetric criteria	
PTV 6000	**D0.1 cm3 < 6420 cGy (+180 cGy)**	**→ Optimal: <6420 cGy, Mandatory: <6600 cGy**
	D5% < 6300 cGy	
	D50% > 5940 cGy	
	D50% < 6060 cGy	
	D98% > 5700 cGy (−120 cGy)	**→ Optimal: >5700 cGy, Mandatory: >5580 cGy**
PTV 4860	D50% > 4860 cGy	
	D98% > 4617 cGy (−97 cGy)	**→ Optimal: >4617 cGy, Mandatory: >4520 cGy**

Fig. 2. Image A demonstrates the clinical plan delivered to the patient on the oncologist's (gold standard) PTV contour. Image B demonstrates the plan created by contours propagated by RIR (the "rigid plan"), on the gold standard PTV contour. The dosimetric coverage of the contours by the rigid plan is then calculated. The anterior aspect of the apex is not covered adequately by the rigid plan (B), highlighted by the arrow. PTV_6000 demonstrated by the pink contour in both images. (For interpretation of the references to colour in this figure legend, the reader is referred to the web version of this article.)
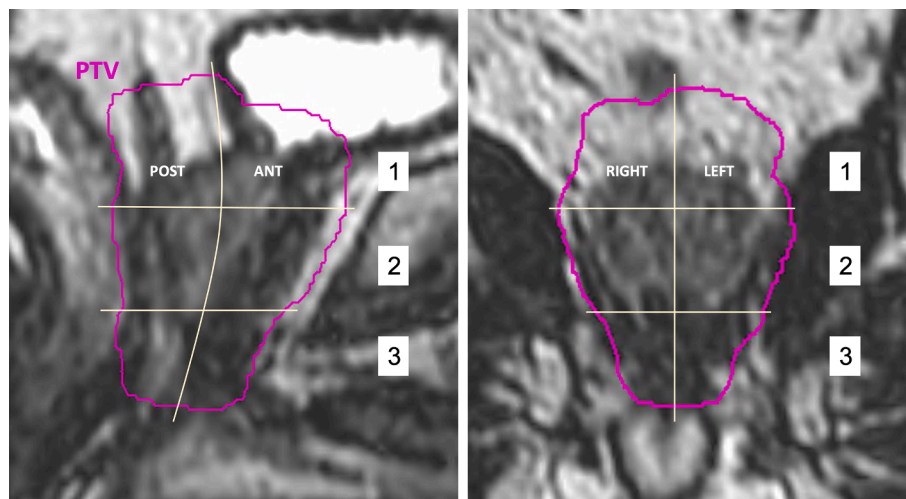

Fig. 3. Sagittal and coronal views are demonstrated. The PTV 6000 was divided into 12 segments visually; superiorly, mid-gland and inferiorly (horizontal slices), anterior-posterior and right-left (vertical slices).

Dose analysis

OARs

For all the deformable and rigid plans analysed (74 plans), the OAR structures always met the mandatory dose constraints.

PTV 4860

The D98% dose target for the secondary PTV (PTV 4860) always met the optimal constraint (4617 cGy). The median D98% dose for the three groups were relatively similar (Fig. 4).

PTV 6000

Regarding dose heterogeneity within the primary PTV 6000 structure, a greater proportion of the rigid plans (74 %) met the optimal target (<6420 cGy) for the D0.1 cc dose constraint than the deformable plans (55 %) (Fig. 4). All rigid and deformable plans met the mandatory target (<6600 cGy) for this dose constraint.

The most important dose objective assessing primary PTV coverage is the D98% > 5700 cGy and this was the most problematic target to achieve with both types of plans (Fig. 4), particularly for the rigid plans.

As a benchmark to compare to, 87 % of the plans used for online treatment met the optimal target for this dose objective, and 100 % met the mandatory target of D98% > 5580 cGy. By comparison, for the plans created from DIR propagated contours, 17 % met the optimal D98% target for coverage of the gold standard contours and this dropped to 3 % of the rigid plans meeting the same target. A greater proportion of rigid plans (55 %) failed to meet the mandatory dose constraint compared to deformable plans (19 %). Overall, the number of clinically acceptable plans were significantly higher with DIR than RIR (p < 0.0001). There was a significant difference seen between the DIR and gold standard groups (p = 0.0046) and between the RIR and gold standard groups (0.0019). These results are reflected in the median dose for D98% outlined in Fig. 4.

The target coverage was very poor in some of the plans. Two deformable plans (5.6 %) and three rigid plans (7.9 %) did not reach the 90 % threshold for coverage of the primary PTV structure with 5700 cGy.

PTV 6000 - D98% > 5700cGy

■ Met Optimum ■ Met Mandatory only ■ Missed Mandatory

Gold standard plans: 86.8, 13.2, 0.0
Deformable plans: 16.7, 63.9, 19.4
Rigid plans: 2.6, 42.1, 55.3

	Median dose (IQR) cGy	
Gold standard	5733 (5714 - 5747)	
Deformable	5630 (5589 - 5668)	
Rigid	5577 (5487 - 5634)	
	Proportion %	
	Satisfactory	Unsatisfactory
Gold standard	100	0
Deformable	80.6 (CI 65-90.2)	19.4 (CI 9.8-35)
Rigid	44.7 (CI 30.1-60.3)	55.3 (CI 39.7-70)

PTV 6000 – D0.1cc < 6420cGy

■ Met Optimum ■ Met Mandatory only ■ Missed Mandatory

Gold standard plans: 78.9, 21.1, 0.0
Deformable plans: 55.6, 44.4, 0.0
Rigid plans: 73.7, 26.3, 0.0

	Median dose (IQR) cGy	
Gold standard	6385 (6359 – 6410)	
Deformable	6409 (6375 – 6446)	
Rigid	6392 (6396 – 6422)	
	Proportion %	
	Satisfactory	Unsatisfactory
Gold standard	100	0
Deformable	100	0
Rigid	100	0

PTV 4860 – D98% > 4617cGy

■ Met Optimum ■ Met Mandatory only ■ Missed Mandatory

Gold standard plans: 100, 0, 0
Deformable plans: 100, 0, 0
Rigid plans: 100, 0, 0

	Median dose (IQR) cGy	
Gold standard	5032 (4996 - 5113)	
Deformable	5096 (4928 - 5249)	
Rigid	5037 (4904 - 5181)	
	Proportion %	
	Satisfactory	Unsatisfactory
Gold standard	100	0
Deformable	100	0
Rigid	100	0

Fig. 4. This figure demonstrates a summary of the PTV 4860 and two PTV 6000 dose objective results. The PTV 6000 D98% dose objective displays the coverage of the gold standard contours whilst the PTV 6000 D0.1 cc reflects where higher doses were delivered. The RIR plans have a higher percentage of missed mandatory and a lower proportion of optimal and mandatory constraints which were met in comparison with the DIR plans. The grey columns represent missed mandatory constraints for D98%, which were seen with both DIR and RIR. The tables demonstrate median dose with interquartile ranges (IQR) achieved for each dose objective for the different plans. A satisfactory plan is one which meets the mandatory target.

PTV coverage

There was a total of 28 out of 74 plans where the D98% > 5700 cGy dose constraint did not meet the mandatory target. Of these, 7 were plans on DIR images and 21 on RIR images. The areas of the PTV 6000 most often not covered by the rigid plans were the bladder/prostate interface and inferiorly at both anterior and posterior borders of the apex. No clear pattern can be seen with the deformable contours (Fig. 5).

Discussion

In this study, we compare dose distributions obtained for automatically propagated prostate contours by deformable or rigid image registration with dose patterns generated from gold standard contours for prostate MR-guided radiotherapy. The strength of the data presented lies in the dosimetric evaluation of the contours, which is more clinically meaningful, rather than the use of geometric indices. Despite geometric
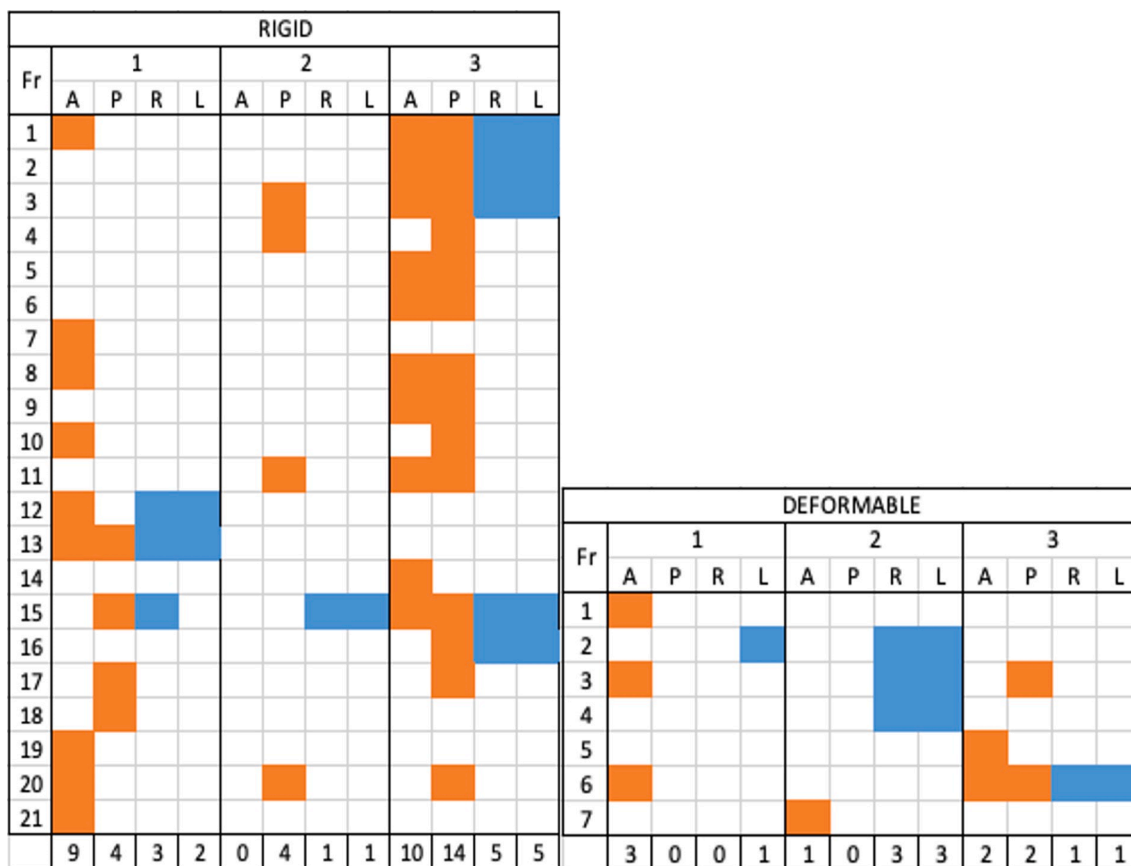
RIGID

Fr	1				2				3			
	A	P	R	L	A	P	R	L	A	P	R	L
1												
2												
3												
4												
5												
6												
7												
8												
9												
10												
11												
12												
13												
14												
15												
16												
17												
18												
19												
20												
21												
	9	4	3	2	0	4	1	1	10	14	5	5

DEFORMABLE

Fr	1				2				3			
	A	P	R	L	A	P	R	L	A	P	R	L
1												
2												
3												
4												
5												
6												
7												
	3	0	0	1	1	0	3	3	2	2	1	1

Fig. 5. Areas of undercoverage of the target for RIR and DIR plans. Segments not covered by the 5700 cGy isodose are displayed in these tables. A = anterior, P = posterior, R = right, L = left. 1 = superior third, 2 = mid third, 3 = lower third. Please refer to Fig. 3. Each row demonstrates a fraction where the mandatory D98% dose constraint for PTV 6000 was missed; a total of 21 rigid plans and 7 deformable plans. The dark orange boxes denote anterior or posterior under coverage whereas the blue represents under coverage laterally. Plans created by RIR predominantly missed the inferior aspect of the prostate (apex) and then the prostate/bladder interface. (For interpretation of the references to colour in this figure legend, the reader is referred to the web version of this article.)

indicators, such as DICE and Hausdorff distance, being the most widely utilised evaluation metrics for contours [21,22], the correlation between geometric and dosimetric indices has been demonstrated to be weak [23,24].

Whilst RIR is comparable to standard non-adaptive radiotherapy, with respect to prostate matching, the coverage of the target, even with MR-image guidance, was found to be poor (45 % of plans were satisfactory). However, due to the presence of the PTV margin, this does not necessarily translate into poor CTV coverage at the time of dose delivery.

With daily adaptation, DIR propagation of the prostate is superior to RIR propagation and 81 % of the time the resultant deformable plan adequately treated the gold standard PTV. This suggests that often, but not always, modification of the prostate contour subsequent to deformable propagation, is unnecessary for target coverage. In practice, our clinical team (including doctors and radiographers) will recontour or amend the prostate contour for every fraction of treatment. Further work is required to identify which of these cases can be adequately treated without any re-contouring.

DIR propagation of the SV, which was the mode of propagation in both the deformable and rigid plans in this study, always resulted in optimal coverage of the PTV 4860 suggesting that DIR propagated SV contours can usually be utilised without modification. However, as the PTV 4860 contains the PTV 6000, the coverage of the distal SV tips may have been compromised in some cases without missing the mandatory coverage objective to the larger volume. This is a limitation of our methodology.

The OAR structures were kept identical to those used online. There was no evidence of systematic overdose to the OARs by using automated

target contours and all the OAR structures met their dose constraints and would be satisfactory for clinical treatment.

The RIR is carried out manually by a treatment radiographer, which means the coverage of the gold standard contours depend on an unavoidable manual element. To assess the reliability of this, a second radiographer carried out the RIR for one fraction from each patient i.e. for a total of ten fractions. There was a very strong positive correlation between the D98% doses for the PTV_6000 for both radiographers (Pearson's coefficient correlation r = 0.95, p < 0.05) and the standard deviation of the change between the two sets of results was 0.7 %. These very similar results suggest that the process was reliable and valid.

Our results for automatic contouring of radiation targets for MRIgRT of prostate cancer are consistent with data in previous studies, although these have largely been CT-based studies. Nourzadeh et al. describe significantly less accurate plans created from autosegmentation of the prostate on CT scans when compared to plans from manually delineated targets [25]. In a study assessing a deep learning autosegmentation tool for MR-based planning, in 35 % of instances prostate contours were considered inadequate and needed manual editing [26]. As technology advances, deep learning is likely to play a larger role in autosegmentation and has been shown to be more accurate when compared to atlas-based techniques [27].

Limitations

The analysis of dose coverage is dependent on how conformal the online plans are, which is a limitation of the study. A good planning solution creates high conformity to the target. At our institution we aim

to create conformal plans which have good OAR sparing whilst remaining robust to contour changes online [20]. Thus if there are differences between the auto-generated contours and clinician defined contours, we would expect to see this reflected in PTV coverage. Despite this, DIR coverage adequately covered the gold standard PTV over 80 % of the time. To ascertain clinical relevance, calculating dose coverage of the prostate CTV on the verification images would have allowed us to determine whether we would retain coverage to the CTV at the time of dose delivery. It is worth bearing in mind that in adaptive radiotherapy, one of the goals is to reduce PTV margins, and thus a higher geometrical accuracy of the propagated contours would be required when compared to standard non-adaptive radiotherapy.

In this study the daily manually drawn contours have been used as the gold standard for comparison. Multiple clinicians are involved in contouring over the course of treatment. Inter- and intra-observer variability is known to exist in prostate radiotherapy for reasons such as clinical experience, image quality and interpretation [21]. This variability is a limitation of this work, as it affects the accuracy of the gold standard contours to which we are comparing the propagated contours. Irrespective, there is no 'true' gold standard, and various contouring studies define the benchmark in different ways. The contours on the reference session image are again susceptible to inter-observer variability, and these inconsistencies can influence the shape of propagated contours and thus the evaluation of plans created from these contours. Further research by eliminating factors that increase the chance of variability would be useful in establishing the true value of automatically propagated contours.

Pathmanathan et al. [28] describes a higher intensity appearance of the prostate with a better defined capsule on T2*W images as compared to the T2W images which are used in this study. A higher consistency of contours are seen on MRI over CT, due to improved soft tissue contrast, and on T2*W images over T2W images [29]. Further work to assess the accuracy of propagated of contours on T2*W images may prove useful for MR-guided RT.

Visual inspection of the 57 Gy isodose mapped on to the PTV 6000 contour to assess coverage is a subjective process. Yet, for the rigid plans a clear pattern of under-dosage at the apex and bladder interface can be seen. The greatest interobserver variability in prostate contouring lies mainly at the apex and base [30,31]. Thus, what is seen in our study is likely to reflect the pre-existing interobserver variability that is present in the reference image contours being translated to the session images when propagated. Staff conducting daily matches should focus on these two areas particularly to reduce the chance of geographical miss, in the absence of adaptive replanning. The location of under-coverage with deformable plans are difficult to predict however the numbers analysed are small.

Accurate automatic contour propagation would significantly strengthen the workflow for MRI-guided radiotherapy for prostate cancer, but this study demonstrates that this cannot be done safely for all cases yet. Further work with greater consensus amongst the gold standard contours is needed and work to assess the dosimetric impact on the prostate CTV itself is warranted.

Conclusion

For patients having daily adaptive radiotherapy on the Unity MR-Linac, we have demonstrated that target volumes propagated by DIR are more accurate than those propagated by RIR. In over four fifths of fractions DIR contours are sufficient to maintain target coverage. Thus, at our institute we have transitioned to DIR propagation of target contours with ongoing online contour editing where necessary. Further research to reduce observer variability, including alternative imaging and improved algorithms for autosegmentation, is required before a contouring free workflow can be recommended.

Appendix A. Supplementary data

Supplementary data to this article can be found online at https://doi.org/10.1016/j.ctro.2022.08.004.

References

[1] McPartlin AJ, Li XA, Kershaw LE, et al. MRI-guided prostate adaptive radiotherapy - A systematic review. Radiother Oncol 2016;119(3):371–80.
[2] Morrow NV, Lawton CA, Qi XS, Li XA. Impact of computed tomography image quality on image-guided radiation therapy based on soft tissue registration. Int J Radiat Oncol 2012;82(5):e733–8.
[3] Posiewnik M, Piotrowski T. A review of cone-beam CT applications for adaptive radiotherapy of prostate cancer. Phys Medica 2019;59:13–21.
[4] Murray J, Tree AC. Prostate cancer – Advantages and disadvantages of MR-guided RT. Clin Transl Radiat Oncol 2019;18:68–73.
[5] Zhang Y, Paulson E, Lim S, et al. A patient-specific autosegmentation strategy using multi-input deformable image registration for magnetic resonance imaging-guided online adaptive radiation therapy: a feasibility study. Adv Radiat Oncol 2020;5(6):1350–8.
[6] Bertelsen AS, Schytte T, Møller PK, Mahmood F, Riis HL, Gottlieb KL, et al. First clinical experiences with a high field 1.5 T MR Linac. Acta Oncol (Madr) 2019;58(10):1352–7.
[7] Raaymakers BW, Jürgenliemk-Schulz IM, Bol GH, Glitzner M, Kotte ANTJ, van Asselen B, et al. First patients treated with a 1.5 T MRI-Linac: clinical proof of concept of a high-precision, high-field MRI guided radiotherapy treatment. Phys Med Biol 2017;62(23):L41–50.
[8] Hwee J, Louie AV, Gaede S, Bauman G, D'Souza D, Sexton T, et al. Technology assessment of automated atlas based segmentation in prostate bed contouring. Radiat Oncol 2011;6(1).
[9] Young AV, Wortham A, Wernick I, Evans A, Ennis RD. Atlas-based segmentation improves consistency and decreases time required for contouring postoperative endometrial cancer nodal volumes. Int J Radiat Oncol 2011;79(3):943–7.
[10] Christiansen RL, Dysager L, Bertelsen AS, Hansen O, Brink C, Bernchou U. Accuracy of automatic deformable structure propagation for high-field MRI guided prostate radiotherapy. Radiat Oncol 2020;15(1).
[11] Njeh CF. Tumor delineation: The weakest link in the search for accuracy in radiotherapy. J Med Phys 2008;33(4):136–40.
[12] Tao C-J, Yi J-L, Chen N-Y, Ren W, Cheng J, Tung S, et al. Multi-subject atlas-based auto-segmentation reduces interobserver variation and improves dosimetric parameter consistency for organs at risk in nasopharyngeal carcinoma: a multi-institution clinical study. Radiother Oncol 2015;115(3):407–11.
[13] Simmat I, Georg P, Georg D, Birkfellner W, Goldner G, Stock M. Assessment of accuracy and efficiency of atlas-based autosegmentation for prostate radiotherapy in a variety of clinical conditions. Strahlentherapie und Onkol 2012;188(9):807–15.
[14] Harrison K, Pullen H, Welsh C, Oktay O, Alvarez-Valle J, Jena R. Machine learning for auto-segmentation in radiotherapy planning. Clin Oncol 2022;34(2):74–88.
[15] Cao X, Yang J, Zhang J, et al. Deformable Image Registration Based on Similarity-Steered CNN Regression. In 2017. p. 300–8.
[16] Prostate Radiotherapy Integrated With Simultaneous MRI (The PRISM Study) [Internet]. [cited 2021 Dec 20]. Available from: https://clinicaltrials.gov/ct2/show/NCT03658525.

[17] Pathmanathan A, Bower L, Creasey H, Dunlop A, Hall E, Hanson I, et al. The PRISM trial- first UK experience of MRI-guided adaptive radiotherapy. Int J Radiat Oncol 2019;105(1):E301.

[18] Winkel D, Bol GH, Kroon PS, van Asselen B, Hackett SS, Werensteijn-Honingh AM, et al. Adaptive radiotherapy: the Elekta Unity MR-Linac concept. Clin Transl Radiat Oncol 2019;18:54–9.

[19] Pathmanathan AU, van As NJ, Kerkmeijer LGW, Christodouleas J, Lawton CAF, Vesprini D, et al. Magnetic resonance imaging-guided adaptive radiation therapy: a "game changer" for prostate treatment? Int J Radiat Oncol Biol Phys 2018;100(2): 361–73.

[20] Dunlop A, Mitchell A, Tree A, Barnes H, Bower L, Chick J, et al. Daily adaptive radiotherapy for patients with prostate cancer using a high field MR-Linac: Initial clinical experiences and assessment of delivered doses compared to a C-arm Linac. Clin Transl Radiat Oncol 2020;23:35–42.

[21] Vinod SK, Jameson MG, Min M, Holloway LC. Uncertainties in volume delineation in radiation oncology: a systematic review and recommendations for future studies. Radiother Oncol 2016;121(2):169–79.

[22] Hanna GG, Hounsell AR, O'Sullivan JM. Geometrical analysis of radiotherapy target volume delineation: a systematic review of reported comparison methods. Clin Oncol 2010;22(7):515–25.

[23] Lim TY, Gillespie E, Murphy J, Moore KL. Clinically oriented contour evaluation using dosimetric indices generated from automated knowledge-based planning. Int J Radiat Oncol Biol Phys 2019;103(5):1251–60.

[24] Kieselmann JP, Kamerling CP, Burgos N, Menten MJ, Fuller CD, Nill S, et al. Geometric and dosimetric evaluations of atlas-based segmentation methods of MR images in the head and neck region. Phys Med Biol 2018;63(14):145007.

[25] Nourzadeh H, Watkins WT, Ahmed M, Hui C, Schlesinger D, Siebers JV. Clinical adequacy assessment of autocontours for prostate IMRT with meaningful endpoints. Med Phys 2017;44(4):1525–37.

[26] Cha E, Elguindi S, Onochie I, Gorovets D, Deasy JO, Zelefsky M, et al. Clinical implementation of deep learning contour autosegmentation for prostate radiotherapy. Radiother Oncol 2021;159:1–7.

[27] Chen W, Li Y, Dyer BA, Feng X, Rao S, Benedict SH, et al. Deep learning vs. atlas-based models for fast auto-segmentation of the masticatory muscles on head and neck CT images. Radiat Oncol 2020;15(1).

[28] Pathmanathan AU, Schmidt MA, Brand DH, et al. Improving fiducial and prostate capsule visualization for radiotherapy planning using MRI. J Appl Clin Med Phys 2019;20(3):27–36.

[29] Pathmanathan AU, McNair HA, Schmidt MA, Brand DH, Delacroix L, Eccles CL, et al. Comparison of prostate delineation on multimodality imaging for MR-guided radiotherapy. Br J Radiol 2019;92(1096):20180948.

[30] Rasch C, Barillot I, Remeijer P, Touw A, van Herk M, Lebesque JV. Definition of the prostate in CT and MRI: a multi-observer study. Int J Radiat Oncol Biol Phys 1999; 43(1):57–66.

[31] McLaughlin PW, Evans C, Feng M, Narayana V. Radiographic and anatomic basis for prostate contouring errors and methods to improve prostate contouring accuracy. Int J Radiat Oncol Biol Phys 2010;76(2):369–78.